Ab initio and DFT Study on 2*H*-Isoxazol-5-one: Consequences of Strong Intermolecular Hydrogen-Bond Formation in Supramolecular Structures

by **Giuseppe Bruno***[a]), **Giovanni Grassi**[b]), **Francesco Nicolò**[a]), and **Roberto Romeo**[c])

[a]) Dipartimento di Chimica Inorganica, Analitica e Chimica Fisica, Università, Vill. S. Agata, I-98166 Messina, (Tel.: +39(090)676-5729, fax: +39(090)393756, e-mail bruno@chem.unime.it)

[b]) Dipartimento di Chimica Organica e Biologica, Università, Vill. S. Agata, I-98166 Messina

[c]) Dipartimento di Farmaco Chimico, Università, Vill. SS. Annunziata, I-98100 Messina

Ab initio and density-functional-theory (DFT) calculations on 2*H*-isoxazol-5-one (A), its linear dimer (LD), cyclic dimer (CD), and cyclic trimer (CT), have been performed with several basis sets in the gas phase, including electron correlation by second-order *Møller-Plesset* perturbation theory. The calculated complexation energy for the intermolecular H-bonded trimer as well as the corresponding geometric changes are in good agreement with the notion of resonance-assisted intermolecular H-bond formation. Bond distances and angles of the optimized geometry of CT are in accordance with the X-ray-diffraction data found on a trimeric supramolecular complex of parent compound 4-(2-methoxybenzyl)-3-phenyl-4*H*-isoxazol-5-one. *Ab initio* and DFT geometry optimizations are also reproducing exactly the large asymmetry in bond angles around the C=O group that is systematically present in all literature available X-ray data for analogous heterocyclic penta-atomic compounds.

Introduction. – Although it is one of the weakest chemical interactions, the H-bond is often the key in supramolecular organization [1][2]; it plays a crucial role in the stabilization of the crystal architectures [3] in the construction of chemical memory devices [4] or even the loss of DNA information [5] so that it plays a determining role in the chemistry of life. Therefore, a better understanding of H-bonding can improve the potential for correlating structure with chemical and biological properties and for designing molecules and then materials with desired properties.

Substituted isoxazol-5-one fragments occur in a large number of compounds [6] which are potential systems for H-bond formation; isoxazol-5-one may exist in three different tautomeric forms, as given in *Fig. 1*.

It was the very strong intermolecular H-bonds observed in the solid state of the N–H tautomeric form of an 4-(arylmethyl) derivative [7] that prompted our interest in studying intermolecular interaction on related models and the complex formation with H_2O and biologically active compounds.

Thus, an *ab initio* and DFT computational study of 2*H*-isoxazol-5-one has been carried out to investigate the nature of intermolecular H-bond formation and its consequences in the rest of the molecule and in a supramolecular aggregate. This is an extension of both our synthetic and structural work on a family of heterocyclic penta-atomic compounds. Full optimization of linear and cyclic dimeric and trimeric supramolecular aggregates was carried out both with *ab initio* (RHF and MP2) and by density-functional (B3LYP) calculations. Single-point-energy calculations (SPE) of the optimized molecules were carried out with several basis sets. The complexation energy

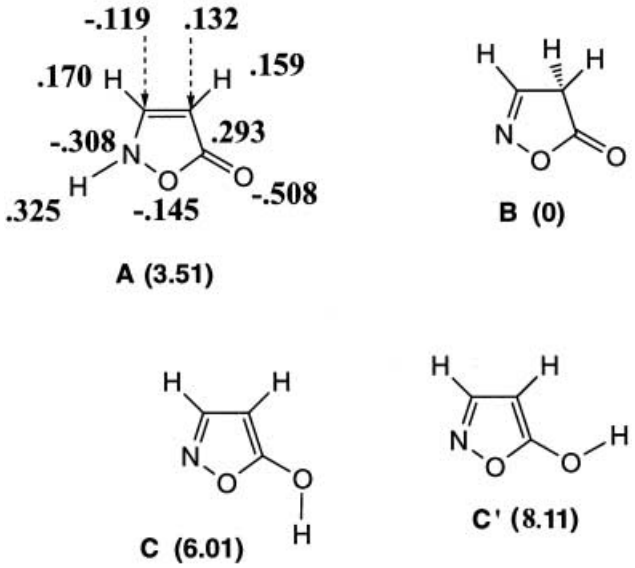

Fig. 1. *Tautomers of* 2H-*isoxazol-5-one.* Relative-stability energies computed at B3LYP/6-31 + G(d,p) level are given in parenthesis. Atomic charges computed at the same level are reported for tautomer A.

has been obtained as the difference between the energy of the corresponding complex and the sum of the energies of the isolated monomer. The computed structural parameters of the cyclic trimer are in excellent agreement with the X-ray determination of a similar supramolecular aggregate of 4-(2-methoxybenzyl)-3-phenyl-4*H*-isoxazol-5-one [7] and are consistent with the notion of resonance-assisted intermolecular H-bond formation (RAHB). Stabilization energies due to the intermolecular H-bond are *ca.* 8.4, 8.5, 18.0, and 34.3 kcal mol^{-1} for linear dimer, cyclic dimer, linear trimer, and cyclic trimer, respectively. Optimized geometries of all models are able to predict the large asymmetry in bond angles around the C=O group experimentally observed in all compounds containing the isoxazol-5-one fragment.

Our aim in this study, however, is more than just checking the strong intermolecular H-bond formation. These studies are an extension of our research of general synthetic and structural determination of heteroconjugated systems, where H-bonds play a fundamental role in determining the production of materials with potential practical applications. There have been other recent crystallographic and computational studies on similar heterocyclic systems [8–10]. Further, we have re-investigated [7] the nature of tautomeric equilibria of 2*H*-isoxazol-5-one (A) that confirms and extends the computational results already reported for this system [10].

Computational Methods. – *Ab initio* (RHF and MP2) and density-functional-theory (DFT) according to the *Becke*'s three-parameter hybrid method (B3LYP) [11][12], molecular modeling, geometry optimization, and single-point-energy (SPE) calculations have been carried out on the monomer, linear dimer (LD), cyclic dimer (CD) and

cyclic trimer (CT) supramolecular complexes of isoxazol-5-one by means of the Gaussian98 [13] series of programs.

Full geometry optimizations of isoxazol-5-one monomer were carried out with basis sets ranging from 6-31G up to 6-311++G(2df,p) at different levels of theory. Due to the size of the systems under investigation, complete optimizations of the geometric structures require considerable computational time. Therefore, the geometry optimizations for the trimeric complex were performed at the HF/6-31G(d), HF/6-31+G, HF/6-31+G(d,p), and B3LYP/6-31+G(d,p) levels; we have not been able to perform more sophisticated calculations on trimeric complexes. All geometries were optimized without symmetry restrictions. The stationary points were confirmed as true minima by frequency. The influence of electron correlation on the geometry of the monomers was evaluated by MP2 geometry optimizations with both the core electrons frozen and including all electrons in the calculations. The atomic charges were calculated by the *Mulliken* population analysis procedure included in the Gaussian98 package. [13] The single-point-energy calculations at several levels of complexity were computed for monomers A1, A2, A3, and for the cyclic trimer CT; the geometry of A1, A2, and A3 was optimized at HF/6-31+G(d,p), MP2(FU)/6-31+G(d,p), and B3LYP/6-31+G(d,p) levels, respectively, while A(T) corresponds to a monomer fragment extract exactly from the optimized trimer at the B3LYP/6-31+G(d,p) level. Calculations were performed by a wide variety of computational methods, which allowed us to determine the relative importance of adding extra diffuse and polarization functions for the study of the influence of H-bonds in determining energy and geometry of the studied system.

Results and Discussion. – As already reported [7][9][10], isoxazol-5-one can exist in four forms shown in *Fig. 1*, consisting of three tautomers and a conformer of 5-hydroxyisoxazole. The stability order was found to be $\mathbf{C}' < \mathbf{C} < \mathbf{A} < \mathbf{B}$, with an energy gap estimated at 8.11 kcal mol^{-1} between **B** and **C**′, while the **C** tautomer in its *syn*-conformation is by 2.1 kcal mol^{-1} more stable than the *anti*-conformer **C**′. For this class of compounds, the nature of solvent was found to have a pronounced effect on tautomeric equilibria [14].

In this paper, we investigated the geometric characteristics of the tautomer **A** and the nature of its peculiar H-bonds in driving self-associations because this tautomeric form was found in the solid state [7].

All optimized equilibrium geometries, energies, and dipole moments of 2*H*-isoxazol-5-one are reported in *Table 1*.

Structures of the tautomer **A** optimized at HF/6-31+G(d,p) (A1), MP2(FU)/6-31+G(d,p) (A2), and B3LYP/6-31+G(d,p) (A3) were also used as starting geometries for single-point-energy calculations at several levels of complexity as well as the cyclic trimer (CT) the geometry of which was optimized at B3LYP/6-31+G(d,p) level. The calculated energy changes for the trimeric association process are summarized in Table 4.

Computational studies on **A** all show a pyramidal N-atom and, consequently, a C_1 symmetry for the molecule. Similar compounds show that, in the solid state, the N-atom in its sp^3 hybridization occurs only when the H-atom bonded to it is not involved in strong H-bonds [15–18]; when a H-bond is present, the sp^2 hybridization of the N-atom is systematically observed [19–21]. The absence of polarized basis set causes a strong

Table 1. *Calculated Geometric Parameters for 2*H-*Isoxazol-5-one*

Parameter	MP2(FC/6-31 + G(d,p)	MP2(Fu)/6-31 + G(d,p)	B3LYP/6-31 + G(d,p)	HF/6-31 + G(d,p)	HF/6-311G(d)	HF/6-31 + G
C(1)=O(1)	1.2162	1.2149	1.2069	1.1829	1.1744	1.2033
C(1)–O(2)	1.4166	1.4143	1.4174	1.3602	1.3594	1.4013
O(2)–N(1)	1.4196	1.4190	1.4098	1.3865	1.3821	1.4143
N(1)–C(3)	1.3855	1.3843	1.3807	1.3853	1.3869	1.3770
C(2)=C(3)	1.3522	1.3503	1.3513	1.3265	1.3228	1.3386
C(1)–C(2)	1.4534	1.4521	1.4551	1.4630	1.4644	1.4529
N(1)–H(1)	1.0167	1.0159	1.0168	1.0008	0.9979	0.9941
C(3)–H(3)	1.0795	1.0785	1.0830	1.0722	1.0717	1.0679
C(2)–H(2)	1.0754	1.0743	1.0784	1.0682	1.0678	1.0641
O(1)=C(1)–O(2)	120.45	120.48	120.28	121.75	121.91	121.03
O(1)=C(1)–C(2)	133.50	133.45	133.82	131.95	131.94	133.07
Δ[a])	13.05	12.97	13.54	10.20	10.03	12.04
C(2)–C(1)–O(2)	106.05	106.07	105.89	106.29	106.15	105.89
C(1)–O(2)–N(1)	107.73	107.74	107.80	109.51	109.66	107.97
O(2)–N(1)–H(1)	107.29	107.23	108.66	107.50	107.31	110.55
O(2)–N(1)–C(3)	106.95	106.92	107.40	106.17	106.16	106.99
C(3)–N(1)–H(1)	117.86	117.77	119.54	116.17	115.52	124.53
N(1)–C(3)=C(2)	110.88	110.89	110.88	111.26	111.23	111.03
C(1)=C(2)–C(3)	107.56	107.57	107.42	106.25	106.28	107.66
Σ < N(1)	332.10	331.92	335.60	329.84	328.99	342.07
μ [Debye]	5.496	5.490	5.692	5.932	5.671	6.681
Energy [au]	– 320.39163	– 320.41714	– 321.28064	– 319.47361	– 319.53124	– 319.30698

[a]) $\Delta = [(O(1)=C(1)–C(2)) – (O(1)=C(1)–O(2))]$.

C(1)=O(1), C(1)–O(2) and O(2)–N(1) lengthening and a large flattening of the N-atom so that its bond-angle sum is 342.07° at HF/6-31 + G level. The introduction of electron correlation appreciably changes the computed values, while there are only marginal differences between full (FU) or frozen-core (FC) MP2 optimizations and DFT calculations. The large variations between the three sets of data (HF with polarized basis set, MP2, and DFT) essentially involve the bond lengths that are more sensitive to the electronic delocalization over the penta-atomic ring than C(1)=O(1), C(1) – O(2), O(2) – N(1), and the C(2)=C(3) bond. So, we observe the C(1)=O(1) length increase from a double-bond character 1.1744 Å (at HF/6-311G(d)) to 1.2162 Å (MP2(FC)/6-31 + G(d,p)); the lengthening is determined by the π-electronic delocalization over the penta-atomic ring. The π-electronic delocalization is also responsible for the C(1)–O(2), O(2)–N(1), and C(2)=C(3) bond lengthening and for the slight shortening of C(2)–C(1).

Bond angles are all within a small range of variation and are in good agreement with several experimental X-ray data reported for analogous compounds [15–21]. Furthermore, all calculations predict the large asymmetry around the C=O C-atom: O(1)–C(1)–O(2) (*ca.*120.4°) and O(1)–C(1)–C(2) (*ca.* 133.5°). This significant asymmetry, as we have already pointed out [22–25], is determined, in the solid state, by both steric and electronic factors; it is systematically observed in all related compounds reported in the *Cambridge Structural Database* (*CSD*) [26].

Dimeric complexes of 2*H*-isoxazol-5-one may be held together by several modes of H-bond interaction. The first group of six linear dimers may be constructed by interaction, as shown in *Fig. 2*, between one of the positively charged H-atoms and one at a time of O-atoms both negatively charged. Obviously, due to the highest charge difference between H(1) and O(1) found at all levels of calculations, which are consistent with the generally accepted NH acidity, the strongest H-bond is the one involving these atoms. As we will discuss later, the strength of the interaction is also governed by its directionality. Since a free rotation around the O···H–X, (X=N,C) is possible, there are a lot of interaction conformers.

There are also six cyclic (CDI – CDVI) and several three-center H-bonded dimeric complexes denoted as DLCI – DLCVI, all depicted in *Fig. 3*.

The optimized geometric parameters for the cyclic dimer (CD) of type IV and VI, and linear dimer (LD) of type I are given in *Table 2*. In *Fig. 4*, *a* we show the numbering scheme adopted, valid for monomers dimers and trimers.

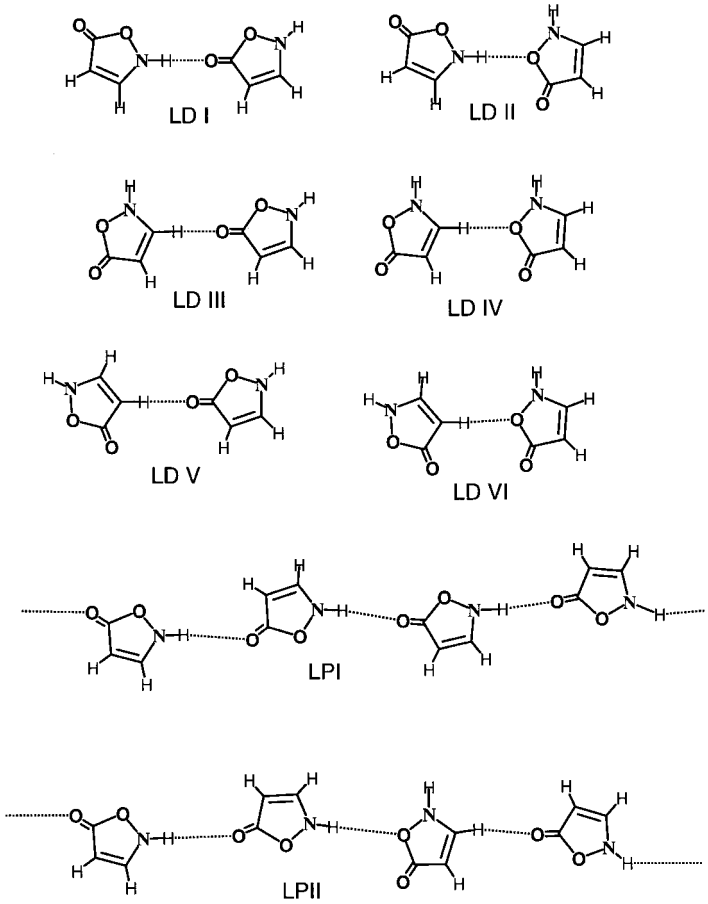

Fig. 2. *Some types of linear complexes of* 2H-*isoxazol-5-one*

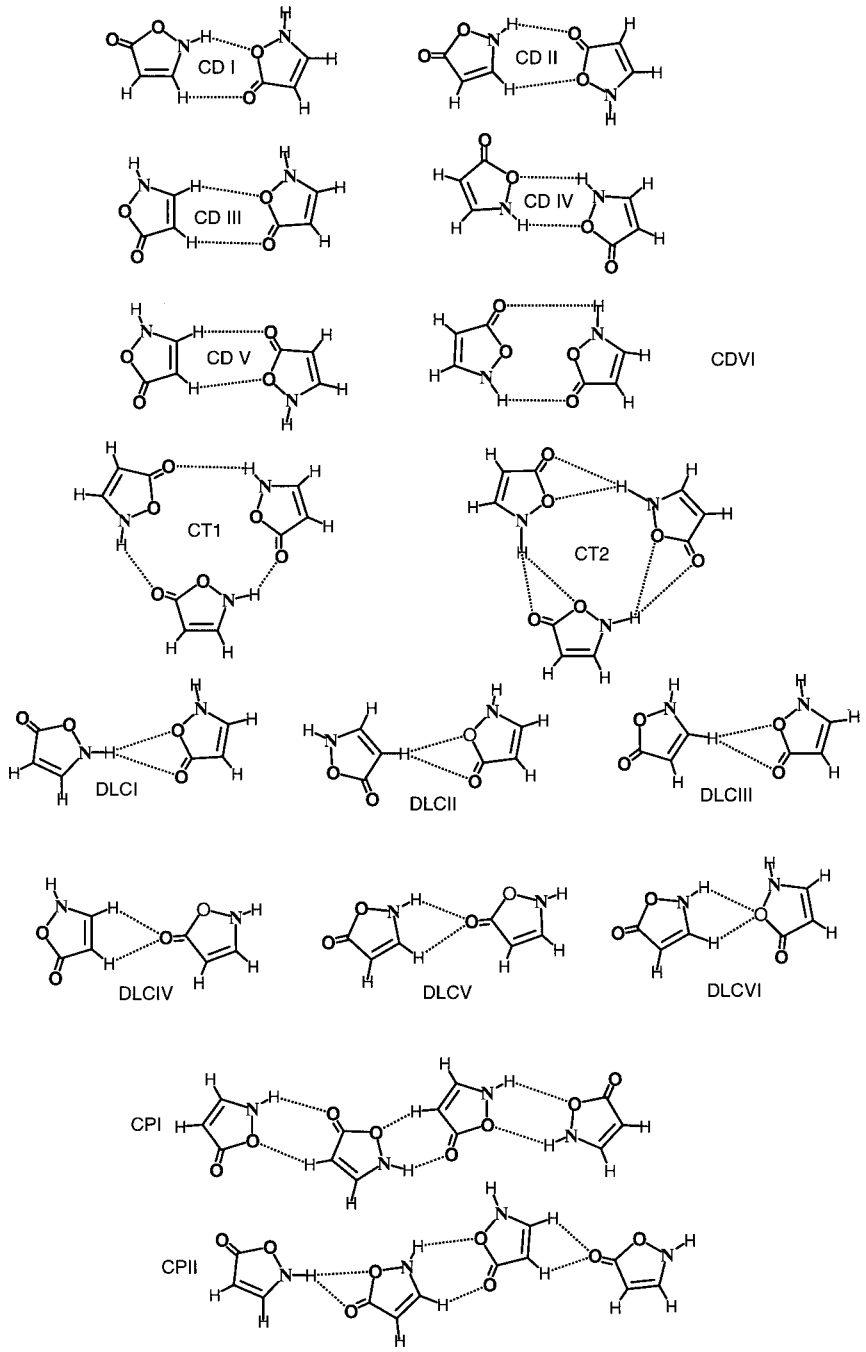

Fig. 3. *Some possible cyclic complexs of* 2H-*isoxazol-5-one*

Table 2. *Calculated Geometric Parameters of Cyclic and Open Dimer of* 2H-*Isoxazol-5-one*

Parameter	HF/6-31 + G(d,p)	B3LYP/6-31 + G(d,p)	MP2(FC)/6-31 + G(d,p)	HF/6-31G(d)	B3LYP/6-31 + G(d,p)	
Complex type	CDIV	CDIV	CDIV	CDVI	LDI	
C(1)=O(1)	1.1871	1.2084	1.2216	1.1905	1.2125	1.2192
C(1)–O(2)	1.3584	1.4253	1.4119	1.3477	1.4167	1.3999
O(2)–N(1)	1.3874	1.4105	1.4200	1.3889	1.4061	1.4038
N(1)–C(3)	1.3809	1.3726	1.3818	1.3835	1.3650	1.3729
C(2)=C(3)	1.3298	1.3558	1.3552	1.3273	1.3589	1.3562
C(1)–C(2)	1.4574	1.4479	1.4470	1.4584	1.4479	1.4452
N(1)–H(1)	1.0029	1.0207	1.0200	1.0050	1.0282	1.0163
O(2)···H(1′)	2.4307	2.1461	2.4017	2.4910[a])	1.8779	(O(1)···H(1′))
O(2)···N(1′)	3.1140	2.9661	2.9780	3.2275[b])	2.9011	(O(1)···N(1′))
O(2)···O(2)	2.9381	3.0157	2.8242	2.9803		
O(1)=C(1)–O(2)	120.78	119.43	119.44	121.43	119.92	119.69
O(1)=C(1)–C(2)	132.81	135.03	134.28	131.92	134.23	133.61
Δ[c])	12.03	15.60	14.84	10.49	14.31	13.92
C(2)–C(1)–O(2)	106.39	105.54	106.27	106.62	105.85	106.71
O(2)–N(1)–C(3)	105.88	107.13	106.66	105.60	107.61	107.64
O(2)–N(1)–H(1)	107.25	108.33	106.86	106.11	110.04	109.29
C(3)–N(1)–H(1)	116.16	121.69	116.91	114.46	122.80	121.69
N(1)–C(3)=C(2)	111.53	111.28	111.15	111.59	111.07	110.60
C(3)=C(2)–C(1)	106.06	107.51	107.29	105.86	107.15	106.85
N(1)–O(2)···H(1′)	124.03	128.70	124.90	106.21[d])	119.76	(C(1)=O(1)···H(1′))
ΣN	329.29	337.15	330.43	326.17	340.45	338.62
μ [Debye]	1.452	0.552	1.501	4.304	7.395	
Energy [au]	–638.96075	–642.57514	–640.80672	–638.92766	–642.57564	

[a]) O(1)···H(1′). [b]) O(1)···N(1′). [c]) Δ = [(O(1)=C(1)–C2)) – (O(1)=C(1)–O(2))]. [d]) C(1)–O(1)···H(1′).

As can be seen from *Table 2*, the computed geometrical parameters as well as the dipole moment shows a large variation because of the large conformational flexibility of the dimeric species.

Linear polymeric structures (LP; *Fig. 2*) of various kinds are also possible for 2*H*-isoxazol-5-one. We have computed the optimized geometry only for linear dimer and trimer of type LDI and LPI at B3LYP/6-31 + G(d,p) level. Geometric parameters as well as the nature of HB interactions in trimeric forms are in good agreement with the geometry of linear dimers; the preferred and strong H-bond interactions were found between N–H and O=C groups. Several kinds of cyclic polymers depicted as CP in *Fig. 3* can exist as elusive species in solution. Full details of the computation with the linear polimeric complex between isoxazol-5-one, in its three tautomeric form, and interesting biological molecules, and the solvent effects are in progress and will be published later.

The supramolecular trimeric aggregate was optimized at the HF/6-31G(d), HF/6-31 + G, HF/6-31 + G(d,p), and B3LYP/6-31 + G(d,p) levels. Complete geometry optimizations required considerable effort; *i.e.*, 65 h with an 1000-MHz PC for the B3LYP/6-31 + G(d,p) computation, so that it was not possible to carry out more-sophisticated calculations. Nevertheless, the results obtained are sufficient to understand the exceptional nature of HB interaction and in reproducing some of the

Table 3. *Calculated Geometric Parameters of Cyclic Trimer of* 2H-*Isoxazol-5-one*

Parameter	B3LYP/6-31 + G(d,p)[a])	B3LYP/6-31 + G(d,p)[b])	HF/6-31 + G(d)[c])	HF/6-31 + G(d,p)[b])	HF/6-31 + G[a])	RX
C(1)=O(1)	1.2387	1.2358	1.1981	1.2011	1.2322	1.231(2)
C(1)–O(2)	1.3994	1.3946	1.3434	1.3423	1.3861	1.389(2)
O(2)–N(1)	1.3812	1.3905	1.3856	1.3826	1.3901	1.392(2)
N(1)–C(3)	1.3325	1.3435	1.3673	1.3632	1.3280	1.334(2)
C(2)=C(3)	1.3809	1.3740	1.3339	1.3379	1.3685	1.371(2)
C(1)–C(2)	1.4217	1.4274	1.4485	1.4471	1.4218	1.410(2)
N(1)–H(1)	1.0515	1.0481	1.0095	1.0099	1.0134	0.935(9)
O(1)···H(1′)	1.6500	1.6843	1.9291	1.9301	1.7708	1.825(9)
O(1)···N(1′)	2.6998	2.7310	2.9308	2.9305	2.7790	2.697(2)
O(2)···O(2′)	3.1484	3.2312	3.6238	3.5511	3.2455	3.151(2)
O(1)=C(1)–O(2)	118.18	118.69	120.62	120.72	118.64	117.6(1)
O(1)=C(1)–C(2)	135.01	134.40	132.03	132.17	134.76	134.2(1)
Δ[d])	16.83	15.71	11.41	11.45	16.12	16.6(1)
C(2)–C(1)–O(2)	106.81	106.90	107.02	107.10	106.59	108.1(3)
O(2)–N(1)–C(3)	109.21	108.33	105.99	106.26	108.49	109.4(9)
O(2)–N(1)–H(1)	114.55	112.49	108.36	109.01	115.38	112.7(9)
C(3)–N(1)–H(1)	136.24	130.18	118.36	119.14	136.13	135.0(9)
N(1)–C(3)=C(2)	110.25	110.61	111.50	111.38	110.63	109.9(9)
C(3)=C(2)–C(1)	106.23	106.21	105.51	105.38	106.49	106.3(9)
C(1)=O(1)···H(1′)	119.05	119.44	117.94	120.85.	121.12	120.1(4)
ΣN(1)	360.00	351.00	332.55	334.41	360.00	357.1(9)
μ [Debye]	0.013	1.853	1.495	3.678	0.001	–
Energy [au]	– 963.89652	– 963.89720	– 968.41536	– 958.46583	– 957.98581	–

[a]) C_{3h}. [b]) C_3. [c]) C_1. [d]) Δ = [(O(1)=C(1)–C(2)) – (O(1)=C(1)–O(2))].

interesting geometric features observed in other parent compounds mentioned above.

As can be seen from an analysis of the optimized geometric parameters reported in *Table 3*, the trimeric supramolecular aggregate may give several conformers, from the planar (C_{3h}) to the almost planar (C_3) and the asymmetric one (C_1), all depicted in *Fig. 4*.

The solid-state X-ray geometries of the parent supramolecular compound 4-(2-methoxybenzyl)-3-phenyl-4*H*-isoxazol-5-one [7] are also included in *Table 3* for comparison.

There are several significant differences between the planar and the folded supramolecular aggregates, and consequently the intermolecular interaction parameters that make resonance in nonplanar disposition impossible over the entire supramolecular aggregate. The trimeric planar aggregate, as well as the slightly distorted one, as confirmed also by the frequency analysis, are not intermediate invertomers but stationary conformers. Reaching planar or folded complexes depends on the level of optimized geometry of monomers used as a starting point to construct the trimeric aggregate for successive minimization and from initial separations of the monomers. Thus, if we start from a monomer optimized at a high level of complexity that successfully reproduces the electron delocalization over the penta-atomic ring, we can easily obtain a planar complex; to do this, we have to start from a monomer

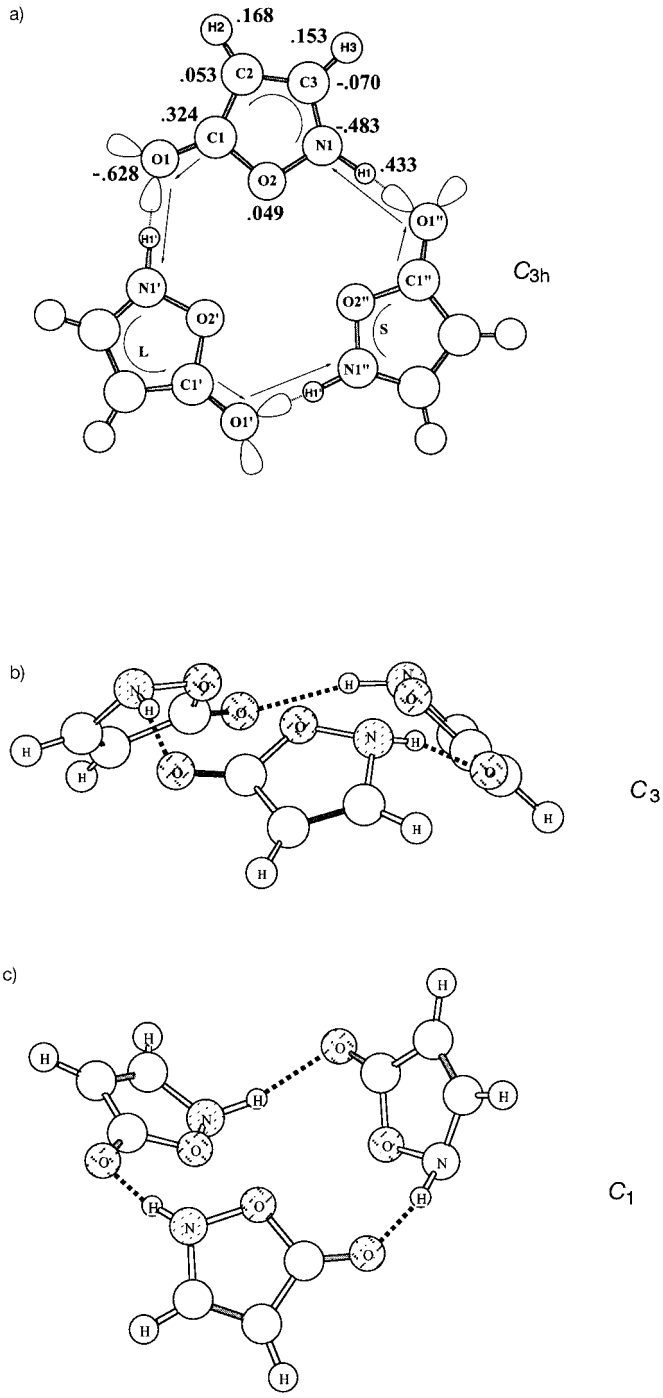

Fig. 4. *Trimeric geometries of* 2H-*isoxazol-5-one:* a) *planar* (C_{3h}), b) *almost planar* (C_3), c) *asymmetric* (C_1). Atomic charges computed at B3LYP/6-31 + G(d,p) level for planar trimeric aggregate are reported for *a*.

optimized at MP(FU)/6-31 + G(d,p) and have performed B3LYP/6-31 + G(d,p). In addition, a planar supramolecular complex can be obtained at several levels of complexity by starting from a trimeric model where the N(1)···O(1′) is less than 2.8 Å. A nonplanar supramolecular aggregate is obtained otherwise. Bond distances and angles within the planar system favor an extended electronic delocalization. This condition, due to the strong RAHB-reinforced N–H···O bonds, can occur *via* 2^3 different pathways, since it can take a long route (L) or a short one (S) on each hetero ring as indicated in *Fig. 4*. The structural parameters computed at B3LYP/6-31G(d,p) level in the penta-atomic ring are in excellent agreement with the corresponding values found in (*S*)-*N*-benzoyl-2-amino-3-(5-oxoisoxazolin-4-yl)propanoic acid [27], (C(1)–C(2): 1.402(2), C(1)–O(2): 1.396(2), C(2)–C(3): 1.372(2), N(1)–C(3): 1.333(2), and N(1)–O(2): 1.384(2) Å) and in our recent X-ray report on the parent compound [7]. The C=O bond distance (1.2387 Å) corresponds to an N···O and a H(1)···O separations of 2.6998 Å and 1.6500 Å, respectively. The N···O separations together with those observed in three enaminones [28] and in the 2-arylpyrazolo[4,3-*c*]quinolin-3-ones [29] are the shortest intermolecular distances so far observed. Nevertheless, in our X-ray report as well in the present computation, we found a corresponding very short C=O distance. Hence, both N···O and C=O distances are surprisingly shorter than any other set of reported values for analogous compounds where π-delocalization enhancement and RAHB are both operating [30].

The angles around the C=O C-atoms (C(2)–C(1)–O(1), α; O(1)–C(1)–O(2), β) show significant asymmetry and have values of 135.01° and 118.18°, respectively. The pronounced difference in the exocyclic angles is determined [22] [31–33] by both steric and electronic factors. It is consistently present in more than 2800 penta-atomic compounds described in the *CSD* that contain the O=C–O fragment (X–C=O (X = C, N), α; O–C=O, β; and O–C–X, γ) The $\Delta\,|\alpha-\beta|$ difference in exocyclic angles is also strongly influenced by the steric effects of the substituents in 2 position, but, in all cases, a significant difference is observed. We observe that, in the monomer A, at all levels of geometry optimizations where steric strains are absent, Δ is *ca.* 12.21°, in good agreement with the solid state reports in *CSD*. Computational results on trimeric aggregate with a nearly C_{3h} symmetry found at HF/6-31 + G and B3LYP/6-31 + G(d,p) levels result in a mean Δ value of 16.47° close to the value of 16.6(1)° found in the X-ray solid state determination [7]. As we have already pointed out [34], this asymmetry is consistently observed, but is, for example, a little less-pronounced because of the slight strain in the coumarin esa-atomic ring.

The calculated total energies and dipole moments computed at different levels for monomers, linear dimer, cyclic dimers, and cyclic trimers are reported in *Tables 1–3*, while, in *Table 4*, we compare the free electronic energy changes for the trimeric association processes. We have computed single-point energy at several levels of complexity starting from the monomers, the geometries of which were optimized with the 6-31 + G(d,p) basis set at HF (A1), MP2(FU) (A2), and B3LYP (A3) chosen, because, at these levels, they show the largest variations in geometric parameters; at the same levels the SPE was also computed for the monomer in its trimer geometry [A(T)] and for the trimer (CT) optimized at B3LYP/6-31 + G(d,p) level. In general, the uncorrected zero-point energy (ZPE) equilibrium binding energies, reported as CT – 3A(T) in *Table 4*, vary considerably with the level of theory used and are observed to

be in the range of 65.49 kcal mol^{-1} (HF/3-21G) to 45.87 kcal mol^{-1} (HF/6-31 + G(d,p)). We observe that, within the HF and MP2 calculations, the introduction of a polarized basis set reduces the binding energies, while the introduction of diffuse functions even on H-atoms does not produce any appreciable reduction. This reduction is dramatically evident, when the basis-set superposition error (BSSE) is taken into account. The BSSE was estimated by the counterpoise procedure (CP) [35] for all trimers in each basis set. The CP-corrected interaction energy of the trimer was obtained by subtracting 3 × individual monomer energies deformation from the trimer energy calculated with the full trimer basis set. The CP-corrected interaction energy is given in *Table 4* as $\Delta E^{\text{CP, Correct}} = (\text{CT} - 3[\text{A(T)} - \text{A3}])$; here, we report the deformation energy required to obtain the monomer geometry as appearing in the trimer $\Delta E_{\text{def}} = [\text{A(T)} - \text{A3}]$ so that the overall CP-corrected interaction energies $\Delta E^{\text{CP,Correct}}$ are given. The enthalpy of the trimerization process, $\Delta H(298\text{ K}) = -48.30$ kcal mol^{-1}, and the *Gibbs* free energy, $\Delta G(29\text{ K}) = -22.21$ kcal mol^{-1}, was obtained from the B3LYP/6-31 + G(d,p) level. Since we do not have experimental results of the interaction energy of 2*H*-isoxazol-5-one, we assume that the value of 34.26 kcal mol^{-1} (32.68 kcal mol^{-1} ZPE-corrected) obtained at B3LYP/6-31 + G(d,p) level may be an adequate energy value in describing the real value of the trimeric association. This value is greater than the value of 22.36 kcal mol^{-1} computed at HF/6-31G(d) level for planar trimeric pyrazole [8], where three N–H···N interactions stabilize the supramolecular aggregate. This analysis suggests another reason for the strong H-bond observed in our supramolecular trimeric complex: the directionality of H-bonds; the mean value of nonbonded angle C=O···H(1) of the interaction of planar complex is 119.94°, identical to the experimental X-ray value. With a systematic survey of the *CSD*, we have

Table 4. *Relative Energies* [kcal mol^{-1}] *for* 2H-*Isoxazol-5-one Trimerization in the Gas Phase*

Method	CT – 3A(T)[a]) ΔE[b])	CT – 3[A(T) – A3][c]) $\Delta E^{\text{CP, Correct}}$[d])	3[A(T) – A3] $3\Delta E_{\text{def}}$	A(T) – A3 ΔE_{def}[e])
HF/3-21G	– 65.49	– 47.25	18.24	6.08
HF/3-21 + G	– 66.15	– 52.77	13.38	4.66
HF/6-31G	– 52.01	– 39.05	12.96	4.32
HF/6-31 + G	– 52.68	– 40.35	12.33	4.11
HF/6-31 + + G	– 53.01	– 40.41	12.60	4.20
HF/6-31G(d)	– 47.51	– 21.47	26.04	8.68
HF/6-31 + G(d,p)	– 45.87	– 22.50	23.37	7.79
HF/6-31 + + G(d,p)	– 45.90	– 22.41	23.49	7.83
MP2/6-31 + G(d,p)	– 57.67	– 38.87	18.80	5.60
MP2/6-31 + + G(d,p)	– 57.37	– 40.72	16.65	5.55
B3LYP/6-31G(d)	– 54.67	– 36.76	17.91	5.97
B3LYP/6-31G(d,p)	– 55.58	– 38.22	17.16	5.72
B3LYP/6-31 + G(d,p)	– 49.32	– 34.26	15.06	5.02
B3LYP/6-31 + + G(d,p)	– 49.30	– 34.24	15.06	5.02

[a]) CT optimized at B3LYP/6-31 + G(d,p) level; A(T) monomer in its trimer goemetry. [b]) $\Delta E = [\text{CT} - 3\text{A(T)}]$, trimerization energy. [c]) A3 Monomer in the B3LYP/6-31 + G(d,p) optimized geometry. [d]) $\Delta E^{\text{CP, Correct}} = (\text{CT} - 3[\text{A(T)} - \text{A3}])$, trimer energy counterpoise-corrected. [e]) ΔE_{def} = Deformation energies required to deform the monomer from its B3LYP/6-31 + G(d, p) optimized geometry to the geometry found in the trimer at the same level.

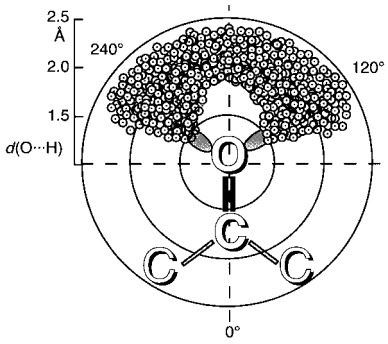

Fig. 5. *CDS Polar scatterplot distribution of X=O ··· H interaction* (C=O ··· H angles *vs.* *d*(O ··· H) distances in the reported C=O group)

identified all intramolecular H-bonds of the C=O group; the results of this research are reported in the polar scatterplot depicted in *Fig. 5*. In the solid state, as was already pointed out [36][37], the preferred approach of the H-atoms toward the C=O O-atoms to form very strong H-bonds are in the lone-pairs directions, *i.e.* the nonbonding angles C=O ··· H are all near 120° for $d(O \cdots H) \leq 1.8$ Å.

Atomic-charge distributions over the atoms for the monomer, calculated by *Mulliken* population analysis directly from the optimized geometry, are reported in *Fig. 1* for monomer A and in *Fig. 4* for trimeric supramolecular complex. The *Mulliken* charges show that the diffuse functions lower the net negative charge on both O-atoms both in the monomeric and trimeric supramolecular aggregate. Diffuse functions on H-atoms have a significant charge increase on H(1) and little influence on H(2) and H(3).

Conclusions. – The main conclusions obtained in this investigation can be outlined as follows: *ab initio* and DFT methods have been used to determine the structures and the interaction energies of 2*H*-isoxazol-5-one, and its dimer and trimer structures in the gas phase. It was found that, in studying the structure of 2*H*-isoxazol-5-one, basis-set and electron-correlation effects are highly significant. Additionally, the results suggest that the geometrical parameters and conformations of trimeric supramolecular aggregates are strongly dependent on the basis sets and from the starting model used. The CT are more stable than the open trimer at any theoretical level of calculations.

The H-bond distances are significantly shorter in the CT compared to the CD or LD, and perfectly reproduce the supramolecular aggregate found in the solid state.

These results demonstrate the usefulness of *ab initio* and DFT calculations in providing a qualitative understanding of the supramolecular self-assembling of 2*H*-isoxazol-5-one.

The results obtained at different levels of complexity indicate that B3LYP density-functional method and HF are equivalent in reproducing geometric parameters of supramolecular aggregate of these kind of systems. On the other hand, the calculated HF H-bonding energy for the CT are underestimated compared to the DFT method. We hope the results provide a valuable picture of the self-association of 2*H*-isoxazol-5-one.

REFERENCES

[1] G. A. Jeffrey, 'An Introduction to Hydrogen Bonding', Oxford University Press New York, 1997.
[2] A. Nangia, G. R. Desiraju, *Acta Crystallogr., Sect. A* **1998**, *54*, 934.
[3] P. Dauber, A. Hagler, *Acc. Chem. Res.* **1980**, *13*, 105.
[4] D. Y. Curtin, I. C. Paul, *Chem. Rev.* **1981**, *81*, 525.
[5] J. A. Sussman, *Mol. Cryst. Liq. Cryst. Sci.* **1972**, *18*, 39.
[6] A. R. Katritzky, C. W. Rees, 'Comprehensive Heterocyclic Chemistry', Elsevier Science Ltd., 1997, Chapt. 4.16, 1 – 130.
[7] G. Grassi, G. Bruno, F. Risitano, F. Foti, F. Caruso, F. Nicolò, *Eur. J. Org. Chem.* **2001**, 4671.
[8] C. Foces-Foces, I. Alkorta, J. Elguero, *Acta Crystallogr.*, *Sect. B* **2000**, *56*, 1018.
[9] S. Woodcock, D. V. S. Gree, M. A. Vincent, I. H. Hillier, M. F. Guest, P. Sherwood, *J. Chem. Soc.* **1992**, 2151.
[10] C. J. Cramer, D. G. Truhlar, *J. Am. Chem. Soc.* **1993**, *115*, 8810.
[11] C. Lee, W. Yang, R. G. Parr, *Phys. Rev. B* **1988**, *37*, 785.
[12] A. D. Becke, *J. Chem. Phys.* **1993**, *98*, 5648.
[13] M. J. Frisch, G. W. Trucks, H. B. Schlegel, G. E. Scuseria, M. A. Robb, J. R. Cheeseman, V. G. Zakrzewski, J. A. Montgomery Jr., R. E. Stratmann, J. C. Burant, S. Dapprich, J. M. Millam, A. D. Daniels, K. N. Kudin, M. C. Strain, O. Farkas, J. Tomasi, V. Barone, M. Cossi, R. Cammi, B. Mennucci, C. Pomelli, C. Adamo, S. Clifford, J. Ochterski, G. A. Petersson, P. Y. Ayala, Q. Cui, K. Morokuma, D. K. Malick, A. D. Rabuck, K. Raghavachari, J. B. Foresman, J. Cioslowski, J. V. Ortiz, A. G. Baboul, B. B. Stefanov, G. Liu, A. Liashenko, P. Piskorz, I. Komaromi, R. Gomperts, R. L. Martin, D. J. Fox, T. Keith, M. A. Al-Laham, C. Y. Peng, A. Nanayakkara, M. Challacombe, P. M. W. Gill, B. Johnson, W. Chen, M. W. Wong, J. L. Andres, C. Gonzalez, M. Head-Gordon, E. S. Replogle, and J. A. Pople, Gaussian, Inc., Pittsburgh PA, 1998.
[14] C. Reichardt, 'Solvents and Solvent Effects in Organic Chemistry', VCH, New York, 1990, 98.
[15] G. Zvilichovsky, *J. Heterocycl. Chem.* **1987**, *24*, 465.
[16] B. Bovio, S. Locchi, *J. Cryst. Mol. Struct.* **1978**, *8*, 149.
[17] R. B. Gammill, S. A. Nash, T. Bell, L. W. Watt, *Tetrahedron Lett.* **1992**, *33*, 997.
[18] M. Atfani, W. D. Lubell, *J. Org. Chem.* **1995**, *60*, 3184.
[19] O. Simonsen, M. L. Hurup Mogelmose, A. La Cour, *Acta Chem. Scand.* **1999**, *53*, 432.
[20] E. Uhlemann, A. Friedrich, G. Hinsche, W. Mickler, U. Schilde, *Z. Naturforsch., B* **1995**, *50*, 37.
[21] S. Tsubotani, Y. Funabashi, M. Takamoto, S. Hakoda, S. Harada, *Tetrahedron* **1991**, *47*, 8079.
[22] F. Risitano, G. Grassi, G. Bruno, F. Nicolò, *Liebigs Ann. Chem.* **1997**, 441.
[23] G. Bruno, F. Nicolò, A. Rotondo, G. Grassi, F. Foti, F. Risitano, C. Bilardo, *Acta Crystallogr.*, *Sect. E* **2001**, *57*, 396.
[24] G. Bruno, F. Nicolò, A. Rotondo, G. Grassi, F. Foti, F. Risitano, C. Bilardo, *Acta Crystallogr.*, *Sect. E* **2001**, *57*, 399.
[25] G. Bruno, G. Grassi, F. Risitano, F. Foti, F. Nicolò, *Heterocycles*, **2001**, 763.
[26] F. H. Allen, J. E. Davies, J. J. Galloy, O. Johnson, O. Kennard, C. F. Macrae, E. M. G. Mitchell, F. Mitchell, J. M. Smith, D. G. Watson, *J. Chem. Inf. Comput. Sci.* **1991**, *31*, 187.
[27] S. Tsubotani, Y. Funabashi, M. Takamoto, S. Hokoda, S. Harada, *Tetrahedron* **1991**, *47*, 8079.
[28] V. Bertolasi, P. Gilli, V. Ferretti, G. Gilli, *Acta Crystallogr., Sect. B* **1998**, *54*, 50.
[29] V. Bertolasi, P. Gilli, V. Ferretti, G. Gilli, *Acta Crystallogr., Sect. B* **1995**, *51*, 1004.
[30] V. Ferretti, V. Bertolasi, G. Gilli, P. A. Borea, *Acta Crystallogr., Sect. C* **1985**, *41*, 107.
[31] G. Bruno, F. Nicolò, A. Rotondo, G. Grassi, F. Foti, F. Risitano, C. Bilardo, *Acta Crystallogr., Sect. E* **2001**, *57*, 396.
[32] G. Bruno, F. Nicolò, A. Rotondo, G. Grassi, F. Foti, F. Risitano, C. Bilardo, *Acta Crystallogr., Sect. E* **2001**, *57*, 399.
[33] G. Bruno, G. Grassi, F. Risitano, F. Foti, F. Nicolò, *Heterocycles* **2001**, 763.
[34] G. Bruno, F. Nicolò, A. Rotondo, G. Grassi, F. Foti, F. Risitano, C. Bilardo, *Acta Crystallogr., Sect. C* **2001**, *57*, 493.
[35] S. F. Boys, F. Bernardi, *Mol. Phys.* **1970**, 553.
[36] F. Allen, C. M. Bird, R. S. Rowland, P. R. Raithby, *Acta Crystallogr., Sect. B* **1997**, *53*, 696.
[37] I. J. Bruno, J. C. Cole, J. P. M. Sommerse, R. S. Rowland, R. Taylor, M. L. Verdonk, *J. Comput.-Aided Mol. Des.* **1997**, *11*, 525.

Received March 15, 2002